POS1-34

Fundamental Study on Resolution Enhancement of Three-Dimensional Imaging in SAR Tomography

Toshihiro Yamada [1], Hiroyoshi Yamada [1], Yoshio Yamaguchi [1]
[1] Graduate School of Science & Technology, Niigata University
Ikarashi 2-8050, Nishi-ku, Niigata-shi, 950-2181 Japan,
tosihiro@wave.ie.niigata-u.ac.jp
yamada@ie.niigata-u.ac.jp

Abstract

In this report, we provide preliminary results of experimental study on resolution enhancement of SAR tomography. The SAR tomography by using repeat-pass SAR images, or multi-baseline observation, can be regarded as a multi-incident angle imaging array technique. Three-dimensional imaging can be realized with these SAR images (baseline data set) by using direction of arrival (DOA) estimation techniques, such as beamforming (BF) method. In the SAR tomography, limited number of base-lines is the most difficult problem. To overcome this difficulty, we propose to apply the Khatri-Rao (KR) product array processing to the SAR tomography which enhance the array aperture and improves the degrees-of-freedom of the array system. Simulation results are provided to show availability of the KR product array processing in SAR tomography. In addition, indoor X-band model experiments were done in an anechoic chamber of our laboratory to demonstrate performance of the proposed processing.

1. Introduction

SAR tomography is a technique to extend the conventional two-dimensional SAR image to three-dimensional representation [1]. Three-dimensional images that include height information are generated by repeat-pass images for the same region with several parallel flight track observations. Obtained data that has been observed by the repeat-path can be regarded as antenna array data. In this report, we demonstrate the analysis by the BF method. In addition, we propose to apply the KR product processing in order to improve the height resolution in the SAR tomography. This technique has been proposed originally for resolution and degrees-of-freedom enhancement of DOA estimation with an array antenna. The KR processing for SAR tomography for height-resolution enhancement is briefly described in the next section.

2. 3D-Imaging by Conventional Beamformer

We first, describe the conventional DOA estimation with array antenna in a repeat-pass monostatic radar briefly. For simplicity, the system is assumed to be a uniform linear array of sensors whose received signal vector can be given by (1), where K is number of incident signals (scattering centers), $s_k(t)$ is the complex amplitude of the signal, and $\boldsymbol{w}(t)$ is the additive white Gaussian noise vector. Moreover, $\boldsymbol{a}(\theta)$ shown in (2) represents the array mode vector, where L is the number of array elements, d is the array element spacing, and $[\cdot]^T$ means transpose. We can derive angular spectrum of the conventional Beamformer defined by (3). In (3), $\boldsymbol{R}$ is the correlation matrix defined by $E[\boldsymbol{x}(t)\boldsymbol{x}(t)^H]$, where $E[\cdot]$ is the ensemble average, and $[\cdot]^H$ is the complex conjugate transpose.

$$\boldsymbol{x}(t) = \sum_{k=1}^{K} \boldsymbol{a}(\theta)s_k(t) + \boldsymbol{w}(t), \tag{1}$$

$$\boldsymbol{a}(\theta) = [1,\ e^{-j\frac{2\pi}{\lambda}2d\sin\theta},\ \cdots,\ e^{-j\frac{2\pi}{\lambda}2(L-1)d\sin\theta}]^T, \tag{2}$$

$$P_{BF}(\theta) = \frac{\boldsymbol{a}(\theta)^H \boldsymbol{R}\, \boldsymbol{a}(\theta)}{\boldsymbol{a}(\theta)^H \boldsymbol{a}(\theta)}. \tag{3}$$

Figure 1 depicts multi-baseline data acquisition processing schematically. The L lines parallel to the height axis show the repeated flight paths. This system can also be said as multi-baseline interferometric SAR. Observing the same region over the L flight paths, L numbers of SAR images can be obtained. When we pick up a pixel at the point (p, q) in each SAR image, we can create the L dimensional array data, $x_l(p, q)$ $(l = 1, 2, \cdots, L)$, by the set of images. This array data vector has the same form as used in the DOA estimation with an array antenna. Hence, Applying the DOA estimation method such as the BF method, we can estimate angular distribution of the scattered signals. In this case, p is the pixel index in the azimuth direction, q is that in the range direction, and the received data vector $\boldsymbol{x}(p, q)$ can be given by

$$\boldsymbol{x}(p, q) = [x_1(p, q), x_2(p, q), \cdots, x_L(p, q)]^T. \tag{4}$$

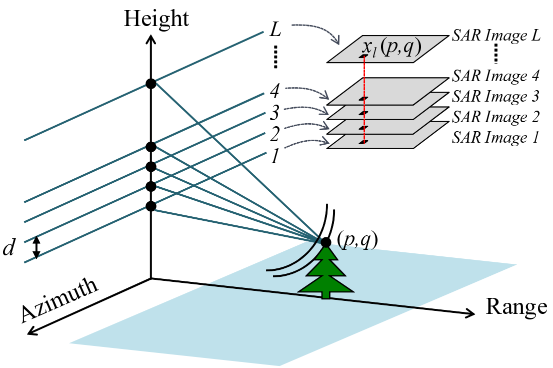

Figure 1: Multibaseline SAR tomography

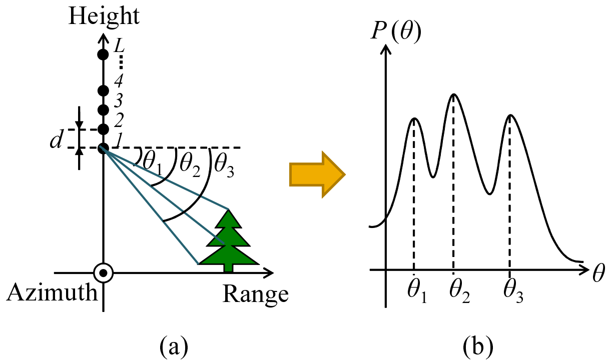

Figure 2: DOA estimation

By using this the received data vector, the BF spectrum defined by (3) can be estimated as shown in Fig. 2(b). The height structure is estimated to transform the angles into the height coordinate (Fig. 2(a)). Since the images are slant-range SLC (Single-Look Complex) images, the estimated spectrum corresponds to the scattering distribution in a circle with a radius of slant-range r_s when center of the reference position is height H. The height of the estimated DOA spectrum at θ can be converted to the ground range r_g and height h information by

$$r_g = r_s \cos\theta, \tag{5}$$
$$h = H - r_s \sin\theta. \tag{6}$$

Three dimensional information of the targets can be estimated by performing above processing at every azimuth and range every pixel in the images.

3. Khatri-Rao Product Array Processing

The KR product is the operation defined by the Kronecker product of columns in two matrices having the same column-dimension. The KR product array processing used in this report can be defined by making a new correlation matrix $\hat{\boldsymbol{R}}$ using the KR product data vector constructed by the conventional data correlation matrix $\boldsymbol{R}$. Degree of freedom of the array can be improved by the KR product array processing [2]. When we assume, in the received data correlation matrix shown in (3), that each incident wave is uncorrelated, then $\boldsymbol{S}$ in (7) becomes a diagonal matrix, therefore (7) holds, where $\odot$ denotes KR product operator, vec$(\cdot)$ is operation which stack each column of the argument matrix to make a vector. In addition, $\boldsymbol{s}$ is a K dimensional column vector consisting of the diagonal elements of $\boldsymbol{S}$. If we redefine (7) as (8), it can be found that the equation (8) has the same form as shown in (1). If we adopt the data vector shown in (8) as a new data vector, we can estimate, or discriminate the signals up to $2(L-1)$ for the uniform linear array having L elements [2], where $\boldsymbol{R}_N$ is the Noise correlation matrix.

$$\begin{aligned}\hat{\boldsymbol{x}} &= \mathrm{vec}(\boldsymbol{R}) \\ &= \mathrm{vec}(\boldsymbol{ASA}^H) + \mathrm{vec}(\boldsymbol{R}_N) \\ &= (\boldsymbol{A}^* \odot \boldsymbol{A})\boldsymbol{s} + \mathrm{vec}(\boldsymbol{R}_N), \quad (7) \\ \boldsymbol{x} &= \boldsymbol{A}_e \boldsymbol{s}_e + \boldsymbol{c}. \quad (8)\end{aligned}$$

4. Simulation Results

In order to confirm the validity of the extension by the KR product showed in the previous section, three-dimensional imaging was performed by computer simulation. Simulation parameters are shown in Table 1. These parameters are selected for the laboratory environment with an anechoic chamber shown in the next section. Point targets were placed in the ground-range direction at intervals 0.025[m] in range 0-5 [m] at 0 [m] height. The results of the target position estimation by simulation are shown in Fig. 3. These are the two-dimensional image for height and grand-range direction at Azimuth direction 1 [m]. As shown in Figs. 3(a) and (b), it can be seen that we can obtain sharp images of the targets by the KR processing and the resolution improvement can be done by the KR product array.

Table 1: Simulation parameters

Center frequency	10.0 [GHz] ($\lambda \fallingdotseq 3.0$ [cm])
Sweep frequency bandwidth	2 [GHz]
Number of sampling frequency points	201
Synthetic aperture length	2.0 [m] ($\fallingdotseq 66.7\lambda$)
Number of azimuthal scanning points	201
Scan interval in azimuth direction	0.01 [m] ($= 1/3\lambda$)
Array aperture length	0.18 [m] ($= 6\lambda$)
Number of height scanning points	13
Scan interval in height direction	0.015 [m] ($= 1/2\lambda$)

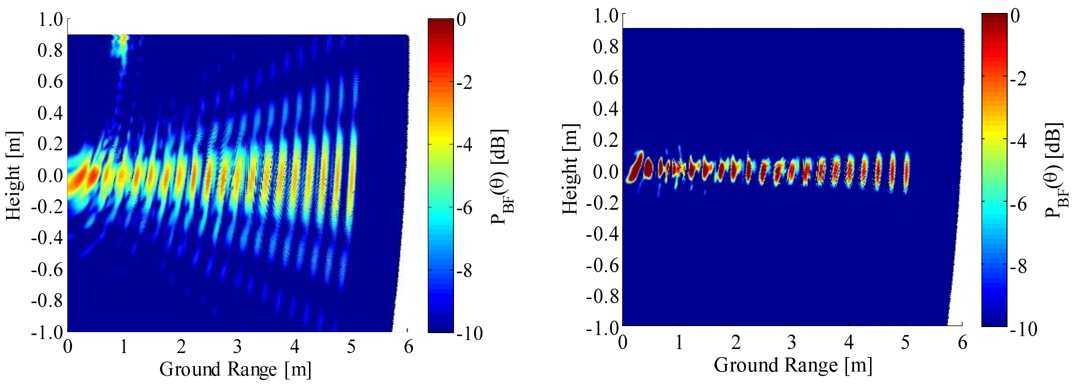

(a) BF without KR processing (b) BF with KR processing

Figure 3: Simulation results of height reflectivity estimation by the BF method

5. Experimental Results

The SAR tomography experiments were carried out by an anechoic chamber. The parameters in the experimental setup is almost the same as shown in Table 1, except for the targets. In this experiment 6 diplanes (corner reflectors) were used. Experimental setup in the laboratory is shown in Figs. 4(a) and (b). This is a preliminary experiment to show the effect of imaging results with and without the KR product processing. The image example obtained by the experiment are shown Fig. 5. These images are the slice image at red broken line plotted in Fig. 4(b). Resolution improvement can be also confirmed in this experiment.

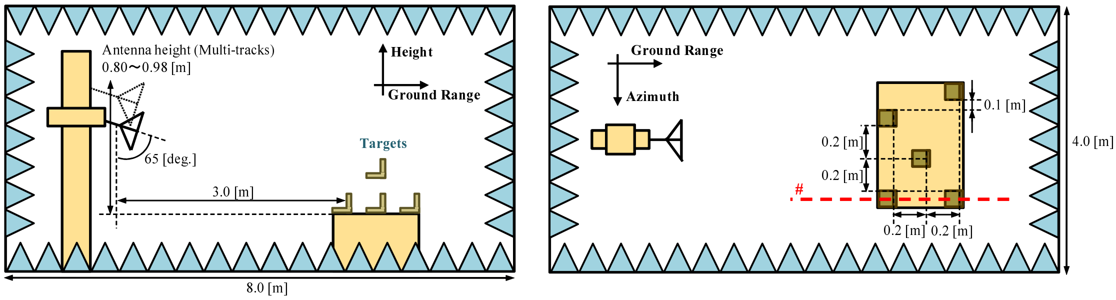

(a) Sideview

(b) Topview

Figure 4: Experimental setup in the anechoic chamber

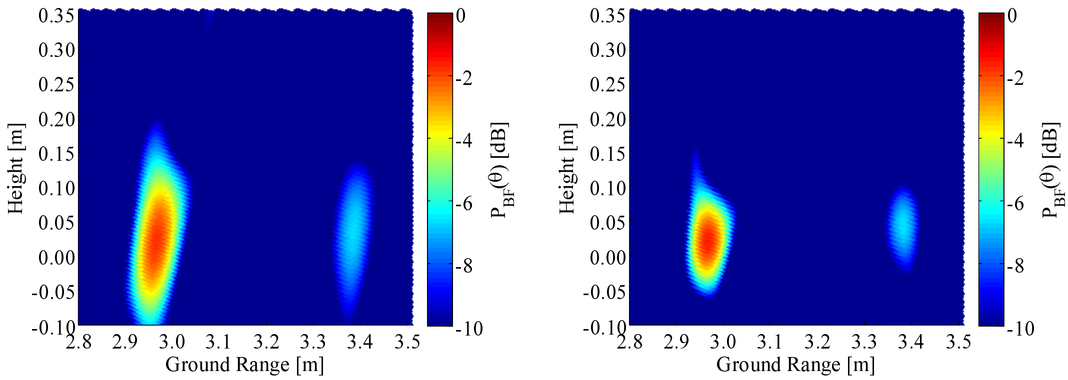

(a) BF without KR processing

(b) BF with KR processing

Figure 5: Preliminary experimental results of height reflectivity estimation by the BF method

6. Conclusions

In this report, we introduced the Khatri-Rao (KR) product array processing used in the DOA estimation method to the SAR tomography. In the introduction, we outlined for the generation of tomographic images by using high resolution DOA estimation technique. In this report, we focused on the resolution improvement by the extended array. We provided the preliminary imaging results of SAR tomography both in simulation and experiment in order to verify the superiority of expansion processing. From these results, it is shown that the improved resolution can be achieved by the processing. In addition to it, the KR approach can improve the degree-of-freedom of the array. This property will be very important for the SAR tomography, and can be also applied with sparse array processing in Compressive-Sensing [3]. This method can be expected to realize much higher resolution capability than that by the BF method, and number of resolvable signals can be also improved. This property will be also studied in near future.

References

[1] A. Reigber and A. Moreira, "First Demonstration of Airborne SAR Tomography Using Multibaseline L-Band Data," IEEE Trans. on Geoscience and Remote Sensing, vol. 38, no. 5, pp. 2142-2152, Sept. 2000.

[2] W. K. Ma, T. H. Hsieh, and C. Y. Chi, "DOA Estimation of Quasi-Stationary Signals With Less Sensors Than Sources and Unknown Spatial Noise Covariance: A Khatri-Rao Subspace Approach," IEEE Trans. Signal Process., vol. 58, no. 4, pp. 2168-2180, Apr. 2010.

[3] D. Malioutov, M. Cetin, and A. S. Willsky, "A Sparse Signal Reconstruction Perspective for Source Localization With Sensor Arrays," IEEE Trans. Signal Process., vol. 53, no. 8, pp. 3010-3022, Aug. 2005.